Environ Sci Pollut Res (2018) 25:8113–8124
DOI 10.1007/s11356-017-9475-6

Testing a ratio of photosynthesis to O_3 uptake as an index for assessing O_3-induced foliar visible injury in poplar trees

Yasutomo Hoshika[1] · Elisa Carrari[1] · Lu Zhang[2] · Giulia Carriero[3] · Sara Pignatelli[1] · Gianni Fasano[4] · Alessandro Materassi[4] · Elena Paoletti[1]

Received: 21 March 2017 / Accepted: 6 June 2017 / Published online: 16 June 2017

Abstract Visible foliar injury by ozone (ozone visible injury) is known as a biomarker to assess potential phytotoxicity of ozone. We investigated ozone visible injury in an ozone-sensitive poplar (Oxford clone) under a 2-year free-air controlled exposure (FACE) experiment and calculated three ozone indices (i.e., accumulative ozone exposure over 40 ppb during daylight hours (AOT40), phytotoxic ozone dose above a flux threshold of 0 nmol m^{-2} s^{-1} (POD_0), and the cumulative value of the ratio of hourly ozone uptake to net photosynthesis ($\Sigma U/P_n$) to assess the critical level (CL) at the time of the first symptom onset of ozone visible injury. We tested the hypothesis that ozone injury depends both on the amount of ozone entering a leaf and on the capacity for biochemical detoxification or repair with photosynthesis as a proxy. The CLs at the time of the first symptom onset of ozone visible injury were 19 ppm h for AOT40, 26 mmol m^{-2} for POD_0, and 1.2 mol mol^{-1} for $\Sigma U/P_n$ in Oxford clone at the ozone FACE experiment. Our findings were then verified by 4-year observation-based data in central Italy on Oxford clone and white poplar (*Populus alba* L.). These observation-based data indicated that we found ozone visible injury in Oxford clone even though AOT40 was relatively low (11.7 ppm h). On the other hand, when values of POD_0 and $\Sigma U/P_n$ exceeded over the CLs, the occurrence of initial symptoms in Oxford clone was shown. White poplar did not show ozone visible injury. $\Sigma U/P_n$ of white poplar at the field sites reached ~1.0 mol mol^{-1} (less than the CL = 1.2 mol mol^{-1}, which was obtained from O_3 FACE) during May–September, although the values of POD_0 were relatively high in white poplar (44–47 mmol m^{-2} during May–September). The result implies that ozone injury may have occurred in poplars when stomatal ozone flux exceeded the critical range of tolerance due to the assimilate shortage for repair and defense against ozone stress.

Keywords Stomatal ozone uptake · Ozone visible injury · Poplars · Oxford clone · White poplar

Responsible editor: Yi-ping Chen

Electronic supplementary material The online version of this article (doi:10.1007/s11356-017-9475-6) contains supplementary material, which is available to authorized users.

✉ Yasutomo Hoshika
yasutomo.hoshika@ipsp.cnr.it

[1] Institute of Sustainable Plant Protection, National Research Council of Italy, Via Madonna del Piano 10, I-50019 Sesto Fiorentino, Italy

[2] College of Horticulture, Northeast Agricultural University, 59 Mucai Street, Harbin 150030, China

[3] Institute of Biometeorology, National Research Council of Italy, Via Giovanni Caproni, 8, 50145 Florence, Italy

[4] Institute of Biometeorology, National Research Council of Italy, Via Madonna del Piano 10, I-50019 Sesto Fiorentino, Italy

Introduction

Tropospheric ozone (O_3) is recognized as a widespread phytotoxic air pollutant, with increasing concentration in the northern hemisphere since pre-industrial times (Hartmann et al. 2013). The phytotoxic nature of O_3 may cause adverse effects on physiological and biochemical processes in trees (Matyssek et al. 2013).

Since the detection of foliar injury by ozone pollution in 1950s (Middleton et al. 1950, 1953, 1956; Haagen-Smit et al. 1952; Noble 1955; Richards et al. 1958), visible foliar injury by O_3 (O_3 visible injury) has been used as a biomarker to assess potential phytotoxicity of O_3. Ozone visible injury has been investigated in native and exotic trees, shrubs, and

herbs and partly validated under controlled conditions in Europe, North and South America, and Asian countries (e.g., Innes et al. 2001; Paoletti et al. 2009a, c; Feng et al. 2014; Moura et al. 2014).

Ozone visible injury does not necessarily represent a serious economic impact to forest trees, such as an impairment of carbon gain (Matyssek et al. 2013). However, O_3 visible injury is the most direct evidence of the harmfulness of current air quality and offers important implications for environmental monitoring and policy processes (Pihl Karlsson et al. 2004).

To assess O_3 risk to trees in Europe, CLRTAP (2015) recommended mainly two methods: (1) a concentration-based index (i.e., accumulated exposure over a threshold of 40 ppb (AOT40) and (2) a stomatal flux-based index (i.e., phytotoxic ozone dose above a threshold Y of uptake (POD_Y), i.e., the accumulated stomatal O_3 uptake over the growing season).

Setting an O_3 critical level (CL) of 5–10 ppm h, AOT40 might be able to protect sensitive tree species from foliar injury (Baumgarten et al. 2000; Van der Heyden et al. 2001; Novak et al. 2003). However, many studies currently suggest that the stomatal flux-based index is more mechanistic because O_3 is harmful to plants only when it is taken up through stomata into leaves (Matyssek et al. 2013; Sicard et al. 2016). Marzuoli et al. (2009) reported that 30 mmol O_3 m^{-2} of POD_0 corresponded to the onset of O_3 visible injury, i.e., the time when injury appears over the growing season, in an O_3-sensitive poplar clone (Oxford: *Populus maximowiczii* Henry × *berolinensis* Dippel) using open-top chambers.

In addition to AOT40 and POD_0, the ratio of stomatal O_3 uptake to net photosynthesis (U/P_n), which indicates a balance between O_3 exposure of mesophyll cells and availability of photosynthates for repair or detoxification, was related to the degree of visible foliar injury in black cherry trees (*Prunus serotina* Ehrh.; Fredericksen et al. 1996). This index may explain O_3 injury to trees better than AOT40 and POD_0 (Kolb and Matyssek 2001; Hoshika et al. 2014).

To answer the question about which is the best index to predict the onset of O_3 visible injury, we examined an O_3-sensitive poplar (Oxford clone) under a 2-year free-air controlled exposure (FACE) experiment and calculated three O_3 indices (i.e., AOT40, POD_0, and $\Sigma U/P_n$, a cumulative value of the ratio of hourly stomatal O_3 uptake to net photosynthesis). We established the CL of these indices corresponding to the first symptom onset of O_3 visible injury. Our findings of CLs were then verified by 4-year field observations on Oxford clone and white poplar (*Populus alba* L.) in central Italy. We thus tested the hypothesis that O_3 injury depends both on the amount of O_3 entering a leaf and on the capacity for biochemical detoxification or repair (with photosynthesis as a proxy; Musselman and Massman 1999; Massman 2004).

Materials and methods

Free-air ozone exposure experiments

The O_3 FACE facility is located at Sesto Fiorentino, near Florence, central Italy (43° 48′ 59″ N, 11° 12′ 01″ E, 55 m a.s.l.). The climate is hot-summer Mediterranean climate according to the Köppen–Geiger classification (Peel et al. 2007). Mean daily temperature during summer (May–September) was 24.0 °C in 2015 and 22.9 °C in 2016. Total precipitation (May–September) was 536.2 mm in 2015 and 226.6 mm in 2016. Ozone was generated from pure oxygen by an O_3 generator (TGOC13X, Triogen Ltd., Glasgow, UK). The air containing O_3 was then diluted with ambient air in a mixing tank and injected into the canopies through 25 teflon tubes hanging down from a fixed grid above the plants (2 m height) in each plot. The O_3 concentration at 2-m height was monitored continuously (Mod. 202, 2B Technologies, Boulder CO, USA), and the observed value was used as feedback to the valves to regulate the O_3 emission, using the proportional–integral–derivative algorithm (PID). Details on the O_3 FACE are described in Paoletti et al. (2017).

The experiments were repeated twice (in 2015 and 2016). Twenty-seven current-year uniform cuttings of O_3-sensitive Oxford poplar clone (*Populus maximoviczii* Henry × *berolinensis* Dippel, courtesy by Marcus Schaub, WSL Birmensdorf, Switzerland) were planted in February 2015 and 2016 in 10 L pots filled with sand/peat/soil = 1:1:1 (*v*/*v*/*v*). In 2015, the plants were exposed to three levels of O_3 concentrations: ambient ozone (AA), ambient ozone ×1.2 (1.2AA), and ambient ozone ×1.4 (1.4AA). To assess the effects of various O_3 exposure levels on poplar plants, in 2016, three different levels of O_3 exposure were tested: ambient ozone (AA), ambient ozone ×1.5 (1.5AA), and ambient ozone ×2.0 (2.0AA). Daily mean O_3 concentration was 35.1, 43.0, and 49.0 ppb at AA, 1.2AA, and 1.4AA, respectively, during the fumigation period in 2015 (from 1 June to 15 October 2015) and 35.0, 51.6, and 66.7 ppb at AA, 1.5AA, and 2.0AA, respectively, during the fumigation period in 2016 (from 1 May to 30 September 2016). We provided three plots per each O_3 treatment and three individuals per plot, with each plot considered as a replicate ($n = 3$). All plants were supplied with water at 1–3-day intervals to avoid water stress.

Field experimental sites

To validate the results of O_3 visible injury obtained by the O_3 FACE experiments, field-observed data in central Italy were used. The first field site was located at Antella (43°44′ N, 11°16′ E). Mean daily temperature and total precipitation during April to October in 2008–2013 were 19.7 °C and 418 mm, respectively (Carriero et al. 2015). In autumn 2007, 1-year-old rooted cuttings of the Oxford clone, raised as explained above

for the FACE experiment, were planted in a line. Each tree was drip irrigated with 1–2 L of water every week to avoid water stress. Soil moisture was measured in the root layer (30-cm depth) by EC5 sensors equipped with an EM5b data logger (Decagon Devices, Pullman, WA, USA). On average, soil moisture was 24.5 ± 0.1% since April to October. The values were near to field capacity (25.5%) for this type of soil, i.e., sandy clay loam. Details of the site are described in Hoshika et al. (2013a) and Carriero et al. (2015). Ozone concentrations were recorded at 2-m height by annually calibrated O_3 monitors (Mod. 202, 2B Technologies, Boulder, CO, USA), i.e., at approximately the same level (1–2 m a.g.l.) where visible injury was surveyed. Daily mean O_3 concentrations were 35.2, 38.4, 35.9, and 33.7 ppb in the year 2008, 2009, 2010, and 2013, respectively, during 1 May to 15 October.

The dataset of white poplar, which is commonly distributed in central Italy, was derived from observations at two field sites. One site was inside the Natural Park of San Rossore near Pisa (43° 43′ N, 10° 20′ E). The other site was located in the shore of Massaciuccoli Lake near the Natural Park of San Rossore. In these sites, three to five naturally growing individual white poplars with 3 to 7-m height were selected as target. The plants grew near a pond at San Rossore, and at the lake side at Massaciuccoli. Therefore, soil water availability was sufficient for those plants. Mean daily temperature and total precipitation during April to October in 2013 were 19.0 °C and 464 mm, respectively, in the Natural Park of San Rossore. Ozone concentrations were recorded at 2-m height by annually calibrated O_3 monitors (Mod. 202, 2B Technologies, Boulder, CO, USA). Daily mean O_3 concentrations were 35.1 and 41.0 ppb at San Rossore and Massaciuccoli, respectively, during 1 May to 15 October 2013.

Ozone exposure indices were calculated from full development of leaves to leaf senescence (May to October). Details are described in "Estimations of ozone indices" section.

Assessment of visible foliar ozone injury

Poplar trees were periodically surveyed over the experimental period in the period 2015–2016 at the O_3 FACE, 2008–2010 and 2013 at Antella, and 2013 at San Rossore and Massaciuccoli. The same two observers assessed leaves of target trees to identify the first onset of O_3 visible injury. All attached leaves were targeted at the O_3 FACE. On the other hand, leaves on fully sun-exposed shoots (three to five shoots per tree) at 1–2-m height were assessed at Antella, San Rossore, and Massaciuccoli field sites. Photoguides were used as described in our previous report (Innes et al. 2001; Paoletti et al. 2009b; Hoshika et al. 2013a). The onset of O_3 visible injury was established when the percentage of visible symptoms was higher than 1% of the surface area of a leaf (Hoshika et al. 2012c). Pest, pathogen, and mechanical injury were not considered in the present study.

Modeling of stomatal conductance and photosynthesis

Diurnal courses of leaf gas exchange were measured using a portable infrared gas analyzer (CIRAS-2 PP Systems, Herts, UK) at the O_3 FACE from April to October 2015 and 2016 and at the other sites from April to October 2013. Leaves with leaf order of four to six from the tip of a shoot, which had a healthy appearance, were measured. Fully sun-exposed shoots (three to five shoots per tree) at 2-m height were targeted at Antella, San Rossore, and Massaciuccoli field sites. During the measurement, the leaf chamber was oriented so as to be fully exposed to the direct irradiance of the sun (Muraoka et al. 2000). The CO_2 concentration in the chamber (C_a) was set to 380 ppm. The temperature in the chamber was adjusted manually to the ambient condition, which was measured by a thermometer under shaded condition at 1.2-m height (Hoshika et al. 2013b). Relative humidity in the leaf chamber tracked the ambient humidity. Pooled data (385 at the O_3 FACE, 330 at Antella, 245 at San Rossore and Massaciuccoli) were used to estimate the parameters of stomatal conductance and photosynthesis models.

Stomatal conductance modeling is often achieved by semi-empirical coupling photosynthesis-stomatal conductance model (e.g., Ball–Woodrow–Berry model; Ball et al. 1987). However, O_3 often causes decoupling of stomatal conductance from photosynthesis (Lombardozzi et al. 2012; Hoshika et al. 2013b). We therefore applied the multiplicative algorithm described by Jarvis (1976) to estimate separately stomatal conductance and photosynthesis. Our stomatal conductance model is based on Hoshika et al. (2012a), as follows:

$$g_{sw} = g_{max} \times f_{phen} \times f_{O3} \times f_{light} \times \max\left\{f_{min}\left(f_{temp} \times f_{VPD} \times f_{SW}\right)\right\}, \quad (1)$$

where gmax is the maximum stomatal conductance (mmol H2O m−2 projected leaf area (PLA) s−1). The other functions are limiting factors of gmax and are scaled from 0 to 1. Here, fmin is the minimum stomatal conductance, fphen is the variation in stomatal conductance with season, and flight, ftemp, fVPD, and fSW depend on photosynthetically relevant photon flux density at the leaf surface (PPFD, μmol photons m−2 s−1), air temperature (T, °C), vapor pressure deficit (VPD, kPa), and volumetric soil water content (SWC, m3 m−3), respectively. fO3 is a response of gsw to O3.

The response of stomatal conductance to phenology (f_{phen}) was described as follows:

for $A_{start} \le DOY < (A_{start} + f_{phen\_a})$,

$$f_{phen} = \left(1 - f_{phen\_c}\right) \times \left((DOY - A_{start}) / f_{phen\_a}\right) + f_{phen\_c}$$

for $(A_{start} + f_{phen\_a}) \le DOY \le (A_{end} - f_{phen\_b})$,
$f_{phen} = 1$;
for $(A_{end} - f_{phen\_b}) < DOY \le A_{end}$,

$$f_{phen} = \left(1 - f_{phen\_d}\right) \times \left((A_{end} - DOY) / f_{phen\_b}\right) + f_{phen\_d}, \quad (2)$$

where DOY is the day of the year. Here, A_{start} and A_{end} are DOY at the start of leaf development (1 April) and the end of the experiment (15 October), respectively. The parameters f_{phen_a} and f_{phen_b} represent the number of days of f_{phen} to reach its maximum and the number of days during the decline of f_{phen} to the minimum value, respectively. The parameters f_{phen_c} and f_{phen_d} represent maximum fraction of f_{phen} at A_{start} and A_{end}, respectively.

The response of g_{sw} to PPFD, i.e., f_{light}, was specified as

$$f_{light} = 1 - \exp(a \times PPFD), \quad (3)$$

where a is a species-specific parameter defining the shape of the exponential relationship.

The parameter for air temperature (T, °C) was expressed as

$$f_{temp} = \left(\frac{T - T_{min}}{T_{opt} - T_{min}}\right) \left\{ \left(\frac{T_{max} - T}{T_{max} - T_{opt}}\right)^{\left(\frac{T_{max} - T_{opt}}{T_{opt} - T_{min}}\right)} \right\}, \quad (4)$$

where T_{opt}, T_{min}, and T_{max} denote the optimum, minimum, and maximum temperature (°C) for g_{sw}, respectively.

The response of g_{sw} to vapor pressure deficit (VPD, kPa) was given by

$$f_{VPD} = \frac{(1 - f_{min}) \times (VPD_{min} - VPD)}{VPD_{min} - VPD_{max}} + f_{min}, \quad (5)$$

where VPD_{min} and VPD_{max} denote the threshold of VPD for attaining minimum and full stomatal opening, respectively. If VPD exceeds VPD_{min}, then f_{VPD} is set to f_{min}. If VPD is lower than VPD_{max}, then f_{VPD} is 1.

The value of f_{O3} was estimated by a linear function of cumulative O_3 uptake (POD_0) (Hoshika et al. 2012b) as follows:

$$f_{O3} = 1 - b \times POD_0, \quad (6)$$

where b is a slope of the linear regression of f_{O3}. The calculation of POD_0 is described in the "Estimations of ozone indices" section.

Terms describing modification of stomatal conductance by the soil moisture (i.e., f_{SW}) were not used in this study. As mentioned above, soil water availability was sufficient because plants were irrigated at O_3 FACE and Antella, and the plants grew near a pond and a lake at San Rossore and Massaciuccoli. No reductions in stomatal conductance due to soil water content were recorded (data not shown).

The photosynthesis model was developed by a similar multiplicative approach (Oue et al. 2011) as follows:

$$P_n = P_{max} \times f'_{phen} \times f'_{O3} \times f'_{light} \times f'_{temp} \times f'_{VPD} \times f'_{SW} - R, \quad (7)$$

where P_{max} is the maximum gross photosynthetic rate (μmol m^{-2} PLA s^{-1}) and R is the respiration rate (μmol m^{-2} PLA s^{-1}). The f' functions are the limiting factors for photosynthesis. The same functional form for effects of environmental factors was adopted for both the stomatal and photosynthesis models except for that of PPFD. This is because stomatal conductance generally reaches a peak sharply at a lower value of PPFD than photosynthesis, which increases more asymptotically (Körner 1995).

The response of photosynthesis to PPFD is expressed as

$$f'_{light} = \left\{ \varphi \times PPFD + 1 - \left[(\varphi \times PPFD + 1)^2 - 4\varphi\theta \times PPFD \right]^{0.5} \right\} / 2\theta, \quad (8)$$

where Φ is the initial slope of the curve and θ is the sharpness in the knee of the curve.

The respiration rate (R) occurs in both light (i.e., R_d*) and dark conditions (i.e., R_d). R_d was obtained from the night-time measurements (22:00 to 23:30). In the model, R above light compensation point of photosynthesis was R_d*, which was assumed to be 50% of R_d (Iio et al. 2004; Watanabe et al. 2014). Temperature dependency of R_d was derived from literature values in hybrid poplars (Fares et al. 2011).

The estimation of parameters (f_{light}, f_{VPD}, f_{temp}) in the models was carried out by a boundary line analysis (e.g., Alonso et al. 2008; Hoshika et al. 2012a, b). First, the g_{sw} and P_n data were divided into classes with the following stepwise increases for each variable: 200 μmol photons m^{-2} s^{-1} for PPFD (when PPFD values were less than 200 μmol photons m^{-2} s^{-1}, PPFD classes at 50 μmol photons m^{-2} s^{-1} steps

were adopted), 2 °C for T, and 0.2 kPa for VPD. A function was fitted against each model variable based on the 95th percentile values per each class of environmental factors. Values of g_{max} and P_{max} were calculated as the 95th percentile and values of f_{min} as the 5th percentile (Alonso et al. 2008).

The function f_{O3} was parameterized using the data of the O_3 FACE. According to Hoshika et al. (2012b), the value of f_{O3} was estimated by a linear regression analysis between daily g_{max} or P_{max} and POD_0. Daily g_{max} or P_{max} was identified as the daily maximum records in the measured trees when PPFD exceeded 500 μmol photons m^{-2} s^{-1}, VPD was less than 1.5 kPa, and T ranged from 20 to 30 °C.

Estimations of ozone indices

AOT40 was estimated by using hourly mean O_3 concentrations during daylight hours (shortwave radiation >50 W m^{-2}, CLRTAP 2015) during the experimental periods (May to October):

$$\mathrm{AOT40} = \sum \max([O_3] - 40, 0), \quad (9)$$

where $[O_3]$ is the hourly mean O_3 concentration (ppb).

Hourly stomatal O_3 flux (F_{st}; nmol m^{-2} s^{-1}) was calculated as

$$F_{st} = [O_3] \times g_{sO3} \times \frac{r_c}{r_b + r_c}, \quad (10)$$

where r_b is the leaf boundary layer resistance (s m^{-1}) and g_{sO3} is the stomatal conductance for O_3 ($g_{sO3} = g_{sw} \times 0.663$; mol m^{-2} PLA s^{-1}); the factor of 0.663 is the ratio of diffusivities between O_3 and water vapor (CLRTAP 2015). Leaf boundary layer resistance (r_b, s m^{-1}) was calculated from the wind speed, u (m s^{-1}), and the cross-wind leaf dimension, L_d (0.04 m, obtained as the mean value of three to five leaves per three to eight trees in each site):

$$r_b = 1.3 \times 150 \times (L_d/u)^{0.5}, \quad (11)$$

where the factor 1.3 accounts for differences in diffusivity between heat and O_3 (CLRTAP 2015).

In Europe, phytotoxic O_3 dose above a flux threshold of Y (POD_Y) was recommended to assess O_3 risk for forest species (CLRTAP 2015). We calculated POD_Y during the experiment (May to October), as follows:

$$\mathrm{POD}_Y = \sum \max(F_{st} - Y, 0), \quad (12)$$

where Y is a species-specific threshold of stomatal O_3 flux (nmol m^{-2} s^{-1}). Sicard et al. (2016) tested Y values for the assessment of O_3 visible injury and found that POD_0 showed the best performance. Therefore, we applied $Y = 0$ nmol m^{-2} s^{-1} here.

To consider a defense component which counteracts O_3 uptake into the leaves, we tested the cumulative value of the ratio of hourly stomatal O_3 uptake to net photosynthesis ($\Sigma U/P_n$), which indicates a balance between O_3 exposure of mesophyll cells and availability of photosynthates for repair or detoxification (Fredericksen et al. 1996; Hoshika et al. 2014). The $\Sigma U/P_n$ (mol mol^{-1}) was accumulated over the growing season (May to October) as

$$\sum U/P_n = \sum (F_{st}/P_n) \quad (13)$$

If P_n was lower than 1 μmol m^{-2} s^{-1}, we did not account for the data so that unrealistic negative values of the ratio were not included.

These three O_3 indices were tested to assess the onset date of the visible injury.

Data analysis

Simple correlation analysis was used to test the relationship between measured and estimated leaf gas exchange (stomatal conductance and net photosynthetic rate). Results were considered significant at $p < 0.05$. All statistical analyses were performed with SPSS software (20.0, SPSS, Chicago, USA).

Results

Ozone visible injury

Ozone visible injury was found in Oxford poplar clone at O_3 FACE and Antella (Table 1). Ozone visible injury occurred as dark stippling on the upper leaf surface, was missing in shaded leaves, and was apparently more severe in older than in younger leaves. Ozone induced the visible injury in July–August at the O_3 FACE. Elevated O_3 treatment at the O_3 FACE hastened the onset of the visible injury (18 July–3 August) compared to ambient treatment. At Antella, Oxford poplar clone showed the visible injury in September–October. On the other hand, we were not able to find O_3 visible injury of white poplar at San Rossore and Massaciuccoli.

Parameterizations of stomatal conductance and photosynthesis models

The g_{max} values for water vapor were set to 520–550 and 360 mmol m^{-2} PLA s^{-1} for Oxford clone and white poplar, respectively (Table 2). The response of g_{sw} to

Table 1 The date of onset of ozone visible injury and corresponding ozone indices for Oxford poplar clone at O_3 FACE and Antella field site and for white poplar at San Rossore and Massaciuccoli field sites

Species and site name, year and treatment	Onset date of visible injury	AOT40 (ppm h)	POD_0 (mmol m^{-2})	$\Sigma U/P_n$
Oxford poplar clone				
O_3 FACE				
Year 2015				
Ambient (AA)	18 August	15.2	23.9	1.07
1.2AA	28 July	17.6	22.5	0.97
1.4AA	28 July	21.6	24.3	1.07
Year 2016				
Ambient (AA)	29 August	9.7	27.2	1.21
1.5AA	3 August	22.5	29.9	1.34
2.0AA	18 July	31.1	32.2	1.35
Antella				
Year 2008	1 September	17.3	33.3	1.48
Year 2009	1 September	18.8	29.7	1.24
Year 2010	7 September	17.1	34.8	1.55
Year 2013	1 October	11.7	34.7	1.38
White poplar				
San Rossore (year 2013)	No injury	–	–	–
Massaciuccoli (year 2013)	No injury	–	–	–

We did not find visible injury in white poplar. Three O_3 indices were tested: accumulative ozone exposure over 40 ppb during daylight hours (AOT40), cumulative phytotoxic O_3 dose above a flux threshold of 0 nmol m^{-2} s^{-1} of stomatal O_3 flux (POD_0), and cumulative value of the ratio of hourly stomatal O_3 uptake to net photosynthesis ($\Sigma U/P_n$)

PPFD (f_{light}) followed a typical light-response curve with a light saturation point above 500 μmol m^{-2} s^{-1} in both poplar species. The response of g_{sw} to air temperature (f_{temp}) indicated that the optimal temperature for stomatal opening did not differ between the species and sites (29–30 °C). A VPD higher than around 1 kPa induced stomatal closure regardless of the species. The correlation coefficient between g_{sw} and POD_0 was statistically significantly different from zero, and 46% of the variation in g_{sw} was explained by POD_0 (Fig. 1).

In the photosynthesis model, the P_{max} values were set to 20.0–20.5 and 19.0 μmol m^{-2} PLA s^{-1} for Oxford clone and white poplar, respectively (Table 3). The response of photosynthesis to PPFD (f'_{light}) indicates that the light saturation point was higher than that of g_{sw} and was around 1000 μmol m^{-2} s^{-1}. The responses of photosynthesis to air temperature (f'_{temp}) and VPD (f'_{VPD}) were similar to those of g_{sw}. Ozone decreased photosynthesis of the Oxford clone, similarly to g_{sw} (Fig. 1). The correlation coefficient between photosynthesis and POD_0 was statistically significantly different from zero, and 72% of the variation in photosynthesis was explained by POD_0 (Fig. 1).

Estimated values of g_{sw} and P_n were in good agreement with the values measured in both poplars (Table 4). The g_{sw} and P models were able to explain 72–83% of the observed g_{sw} and P_n variance.

Test of ozone indices for assessing the onset of ozone visible injury

We calculated three O_3 indices to find the corresponding values for the first symptom onset of O_3 visible injury in Oxford poplar clone at O_3 FACE (Table 1, Fig. 2). All O_3 indices during May to September at all sites are shown in supplementary information (Table S1). Different AOT40 values (min–max 9.7–31.1 ppm h) were observed between O_3 treatments at O_3 FACE at the time when the first symptom was observed. In 2015, the AOT40 corresponding to the onset of O_3 visible injury was 42% higher in 1.4AA than in AA. In 2016, even larger differences of AOT40 values at the onset date of visible injury were found between O_3 treatments (+220% in 2.0AA relative to AA). On the other hand, regardless of O_3 treatments, similar POD_0 and $\Sigma U/P_n$ were required for the onset of visible injury at O_3 FACE. The averaged values of these indices at the onset date of O_3 visible injury were 19 ppm h AOT40, 26 mmol m^{-2} POD_0, and 1.2 mol mol^{-1} $\Sigma U/P_n$. These values may be suggested as the CL corresponding to the first symptom onset of O_3 visible injury.

The CLs obtained from O_3 FACE were then verified by the data on Oxford clone and white poplar in central Italy (at Antella, San Rossore, and Massaciuccoli; Table 1; Fig. 3). The occurrence of initial symptoms in Oxford clone at

Table 2 Summary of Jarvis-type stomatal conductance model parameters for Oxford poplar clone and white poplar

Parameter			Oxford poplar clone O_3 FACE	Antella	White poplar
g_{max}	(mmol H_2O m^{-2} PLA s^{-1})		520	550	360
f_{min}		(fraction)	0.08	0.10	0.09
f_{phen}	A_{start}	(day of year)	91	91	91
	A_{end}	(day of year)	304[a]	334	334
	f_{phen_a}	(days)	19	36	55
	f_{phen_b}	(days)	24	36	80
	f_{phen_c}	(fraction)	0.2	0.2	0.2
	f_{phen_d}	(fraction)	0.2	0.2	0.2
f_{light}	a	(constant)	−0.0021	−0.0039	−0.0036
f_{temp}	T_{opt}	(°C)	29	29	30
	T_{min}	(°C)	5	5	5
	T_{max}	(°C)	45	40	40
f_{VPD}	VPD_{max}	(kPa)	1.3	1.2	1.2
	VPD_{min}	(kPa)	5.9	4.4	4.5
f_{O3}	b	(constant)	0.0098	0.0098[b]	Not applied

g_{max} is the maximum stomatal conductance; f_{min} is a fraction of minimum stomatal conductance to g_{max}; f_{phen} is the the variation of stomatal conductance with season; f_{light}, f_{temp}, f_{VPD}, and f_{O3} depend on photosynthetically relevant photon flux density at the leaf surface (PPFD, μmol m^{-2} s^{-1}), temperature (T, °C), vapor pressure deficit (VPD, kPa), and phytotoxic O_3 dose (POD_0, mmol m^{-2}), respectively; A_{start} and A_{end} are the year days for the start of leaf development and for the leaf fall, respectively; f_{phen_a} and f_{phen_b} represent the number of days of f_{phen} to reach its maximum and the number of days during the decline of f_{phen} to the minimum value, respectively; f_{phen_c} and f_{phen_d} represent maximum fraction of f_{phen} at A_{start} and A_{end}, respectively; a is the parameter determining an exponential curve of stomatal response to light; T_{opt}, T_{min}, and T_{max} denote optimal, minimum, and maximum temperature for stomatal opening, respectively; VPD_{min} and VPD_{max} denote the threshold of VPD for attaining minimum and full stomatal opening, respectively; b is the slope parameter of the relationship between stomatal conductance and POD_0

[a] A_{end} was set as the date for the end of the experiment

[b] b was set as the same value obtained from O_3 FACE experiment

Antella was shown above the CLs of POD_0 and $\Sigma U/P_n$ (Table 1). Even though AOT40 was relatively low (11.7 ppm h), we found ozone visible injury in Oxford clone.

We then tried to predict the onset date by using the CLs. If we assumed the occurrence of initial symptoms when each index exceeded over the CL, $\Sigma U/P_n$ could reproduce the onset date of O_3 visible injury better than that of POD_0 (Fig. 3, $R^2 = 0.54$ in $\Sigma U/P_n$ and $R^2 = 0.12$ in POD_0). AOT40 could not reproduce the onset date of O_3 visible injury because AOT40 did not reach the CL (19 ppm h) during the growing season 2008, 2010, and 2013 at Antella (Table S1).

White poplar did not show O_3 visible injury. $\Sigma U/P_n$ of white poplar did not exceed ~1.0 mol mol^{-1} during May–September, although POD_0 values were relatively high in white poplar (44–47 mmol m^{-2} during May–September) (Table S1).

Discussion

Symptoms of O_3 visible injury were assessed at the O_3 FACE. Ozone visible injury at near-ambient level of O_3 concentration may slowly develop over several months, exhibiting stippling

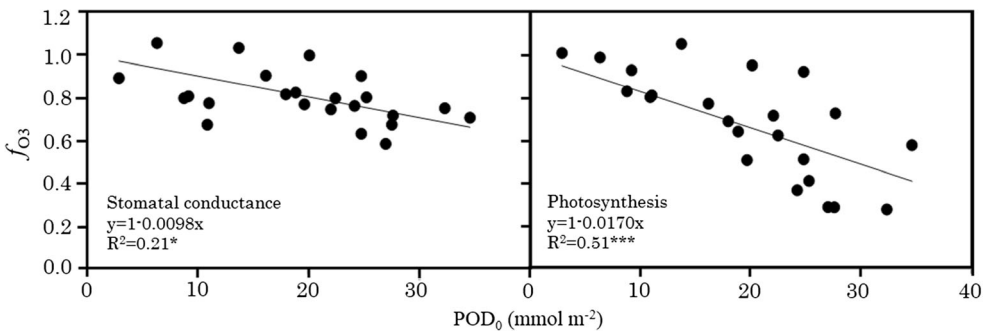

Fig. 1 Relationships between phytotoxic O_3 dose above a flux threshold of 0 nmol m^{-2} s^{-1} of stomatal O_3 flux (POD_0) and relative stomatal conductance (*left figure*) or photosynthesis (*right figure*) in Oxford poplar clone. Regression analysis: *$p < 0.05$; ***$p < 0.001$

Table 3 Summary of Jarvis-type photosynthesis model parameters for Oxford poplar clone and white poplar

Parameter			Oxford poplar clone O_3 FACE	Antella	White poplar
P_{max}	(μmol CO_2 m^{-2} PLA s^{-1})		20.0	20.5	19.0
R_{d25}	(μmol CO_2 m^{-2} PLA s^{-1})		1.7	1.3	1.8
f'_{phen}	A_{start}	(day of year)	91	91	91
	A_{end}	(day of year)	304[a]	334	334
	f_{phen_a}	(days)	40	25	45
	f_{phen_b}	(days)	85	69	69
	f_{phen_c}	(fraction)	0.2	0.2	0.2
	f_{phen_d}	(fraction)	0.2	0.2	0.2
f'_{light}	Φ	(constant)	0.0020	0.0015	0.0012
	θ	(constant)	0.86	0.92	0.94
f'_{temp}	T_{opt}	(°C)	27	29	29
	T_{min}	(°C)	5	5	5
	T_{max}	(°C)	46	40	40
f'_{VPD}	VPD_{max}	(kPa)	1.5	1.8	1.9
	VPD_{min}	(kPa)	6.0	5.1	7.0
f'_{O3}	b	(constant)	0.0170	0.0170[b]	Not applied

P_{max} is the maximum gross photosynthetic rate; R_{d25} is the dark respiration rate at 25 °C; f'_{phen} is the variation of photosynthesis with season; f'_{light}, f'_{temp}, f'_{VPD}, and f'_{O3} depend on photosynthetically relevant photon flux density at the leaf surface (PPFD, μmol m^{-2} s^{-1}), temperature (T, °C), vapor pressure deficit (VPD, kPa), and phytotoxic O_3 dose (POD_0, mmol m^{-2}), respectively; A_{start} and A_{end} are the year days for the start of leaf development and for the leaf fall, respectively; f_{phen_a} and f_{phen_b} represent the number of days of f_{phen} to reach its maximum and the number of days during the decline of f_{phen} to the minimum value, respectively; f_{phen_c} and f_{phen_d} represent maximum fraction of f_{phen} at A_{start} and A_{end}, respectively; Φ and θ are the initial slope of the light-response curve and the sharpness of the knee of the curve, respectively; T_{opt}, T_{min}, and T_{max} denote optimal, minimum, and maximum temperature for photosynthesis, respectively; VPD_{min} and VPD_{max} denote the threshold of VPD for attaining minimum and maximum photosynthesis, respectively; b is the slope parameter of the relationship between photosynthesis and POD_0

[a] A_{end} was set as the date for the end of the experiment

[b] b was set as the same value obtained from O_3 FACE experiment

and cell alterations such as cell wall thickening, pectinaceous projections, and changed vacuolar content (Günthardt-Goerg et al. 2000). As we expected, elevated O_3 condition at O_3 FACE hastened the onset of the visible injury. Previous observations of O_3 visible injury in Europe indicated an O_3 CL of 5–10 ppm h AOT40 for the protection of sensitive tree species from visible injury (Baumgarten et al. 2000; Van der Heyden et al. 2001; Novak et al. 2003). In the present study, although the CL was set to 19 ppm h AOT40 for the onset of O_3 visible injury, even less AOT40 (~10 ppm h) was observed at the time of the occurrence of initial foliar symptom (Table 1; in AA treatment at O_3 FACE in 2015, at Antella in 2013). Setting an AOT40-based CL might be useful to protect the most sensitive species under the most sensitive environmental conditions (level I assessments; CLRTAP 2015). However, the degree of exceedance may not provide a measure of the relative risk of O_3 visible injury. In fact, a much higher value of AOT40 (31.1 ppm h) was required for the onset of O_3 visible injury in 2.0AA at O_3 FACE in 2016 (Table 1). Sicard et al. (2016) demonstrated that AOT40 did not correlate with O_3 visible injury in southern European forests. To estimate the quantitative effects of O_3 on plants (level II assessments; CLRTAP 2015), the effects of environmental and physiological factors on the plant response to O_3 have to be taken into account (Paoletti and Manning 2007; Matyssek et al. 2013).

Many studies have currently recommended the stomatal flux-based approach because O_3 is injurious to plants only after it is taken up through stomata into leaves (Matyssek et al. 2013).

Table 4 Results of the correlation analyses between measured and estimated stomatal conductance values by using the Jarvis-type stomatal conductance (g_s model) and photosynthesis models (P model) for Oxford poplar clone (at O_3 FACE and Antella) and white poplar

Species (and place)	g_s model	P model
Oxford poplar clone		
O_3 FACE (n = 90)	R^2 = 0.72	R^2 = 0.83
	RMSE = 86.3	RMSE = 3.8
	$y = 0.94x - 0.0018$	$y = 0.74x - 0.053$
	$p < 0.001$	$p < 0.001$
Antella (n = 42)	R^2 = 0.83	R^2 = 0.81
	RMSE = 65.2	RMSE = 3.2
	$y = 0.81x + 0.070$	$y = 0.74x + 0.87$
	$p < 0.001$	$p < 0.001$
White poplar (n = 20)	R^2 = 0.75	R^2 = 0.83
	RMSE = 51.9	RMSE = 3.3
	$y = 0.80x + 0.031$	$y = 1.02x + 2.07$
	$p < 0.001$	$p < 0.001$

The R^2 values and linear regressions were determined using averages of one round of measurements (in three plots at O_3 FACE and in three to five trees at the other sites)

RMSE root mean square error (unit: mmol m^{-2} s^{-1} for g_s model, μmol m^{-2} s^{-1} for P model)

Many studies have currently recommended the stomatal flux-based approach because O_3 is injurious to plants only after it is taken up through stomata into leaves (Matyssek et al. 2013).

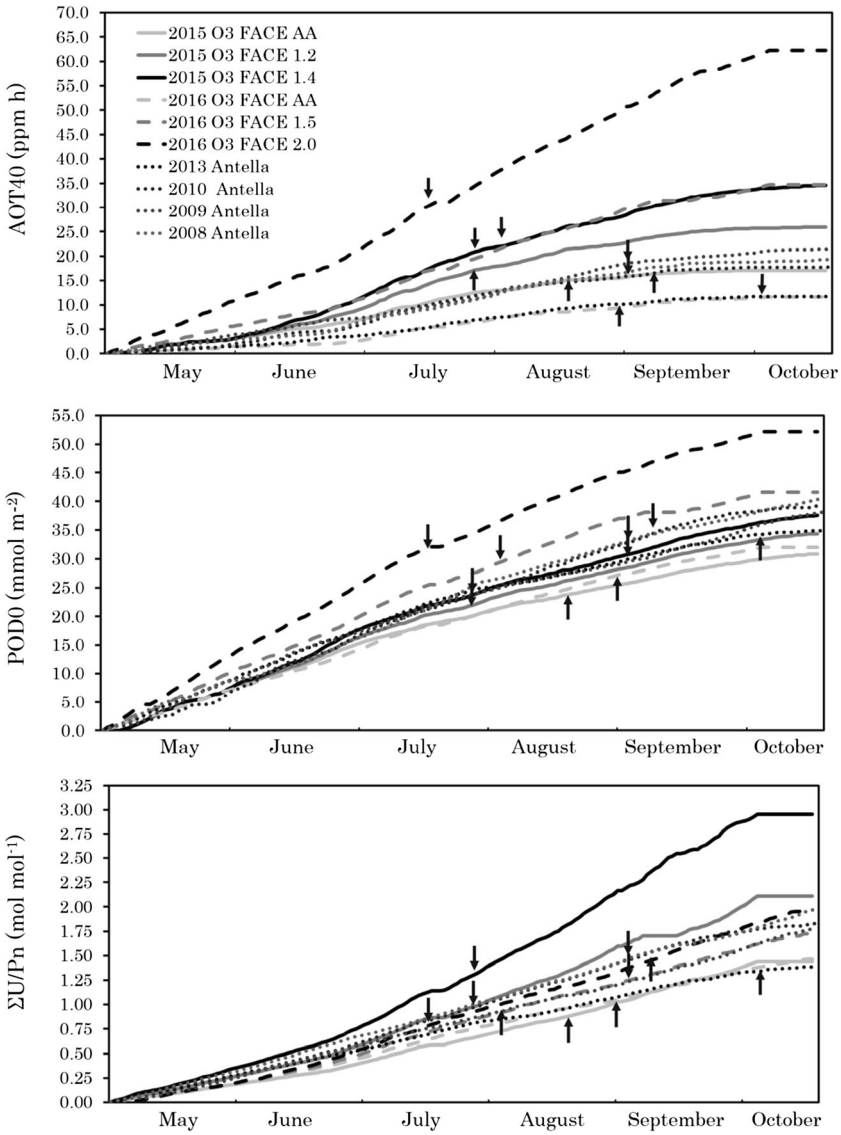

Fig. 2 Relationships between O_3 indices and the onset date of O_3 visible injury for Oxford poplar clone. Three O_3 indices were tested: accumulative ozone exposure over 40 ppb during daylight hours (AOT40; *top figure*), phytotoxic O_3 dose above a flux threshold of 0 nmol m^{-2} s^{-1} of stomatal O_3 flux (POD_0; *center figure*), and cumulative value of the ratio of hourly stomatal O_3 uptake to net photosynthesis ($\Sigma U/P_n$; *bottom figure*). The *arrows* denote the onset of O_3 visible foliar injury. Please see Table 1 for details

POD_0 values corresponding to the first symptom onset of O_3 visible injury in Oxford clone were similar among O_3 treatments at O_3 FACE (Table 1; Fig. 2). According to our results, 26 mmol O_3 m^{-2} of POD_0 corresponded to the onset of O_3 visible injury. This value was similar to the values in *Fagus sylvatica* (25 mmol m^{-2} in the field observation, Sicard et al. 2016) and in the same Oxford clone (30 mmol m^{-2} by an open-top chamber experiment, Marzuoli et al. 2009). The result indicates that POD_0 was high enough for the onset of O_3 visible injury even when the AOT40 was relatively low (e.g., in 2013 at Antella).

Ozone injury may depend both on the amount of O_3 entering a leaf and on the capacity for biochemical detoxification or

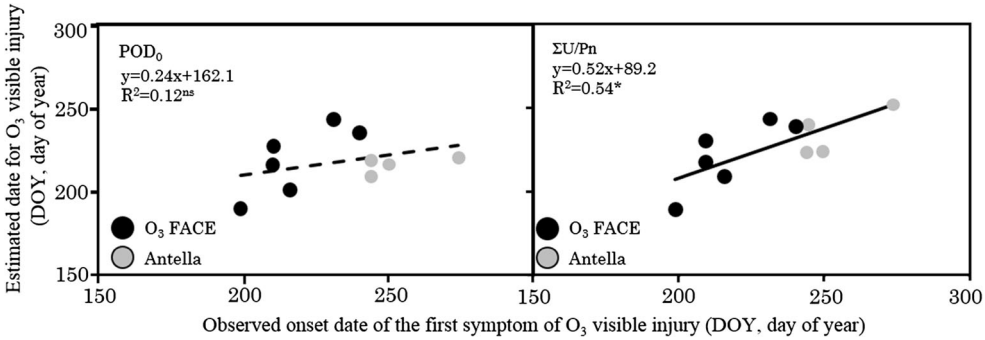

Fig. 3 Comparison between the onset dates of visible injury of Oxford poplar clone as estimated by the critical levels using POD0 (*left figure*) and $\Sigma U/P_n$ (*right figure*) critical levels and as observed at O_3 FACE (years 2015 and 2016) and Antella field site (years 2008–2010, 2013). Regression analysis: $*p < 0.05$; *ns* not significant

repair (Matyssek et al. 2008; Hoshika et al. 2014). To assess O_3 visible injury, we innovatively tested $\Sigma U/P_n$. According to our results, 1.2 mol mol^{-1} of $\Sigma U/P_n$ could be suggested as the CL value for the onset of O_3 visible injury. If we tried to predict a date of initial symptoms when a value of index exceeded over the CL, $\Sigma U/P_n$ could reproduce the onset date of O_3 visible injury better than that of POD_0 (Fig. 3). Musselman and Massman (1999) suggested the defense of plants to O_3 to be related to photosynthesis because detoxification and repair need energy, and this may be provided by the photosynthates (Smirnoff 1996; Noctor and Foyer 1998). In the present study, we found that O_3 visible injury was more severe in middle-aged and older leaves than younger leaves. Older leaves generally had a lower photosynthetic capacity (e.g., Hoshika et al. 2013b) than younger leaves, suggesting a lower availability of photosynthates for detoxification and repair (Pihl Karlsson et al. 1995). This suggests that O_3 visible injury may have finally occurred in poplars when stomatal O_3 uptake exceeded the critical range of tolerance due to the assimilate availability for repair and defense against O_3 stress.

In white poplar, we did not find the O_3 visible injury at the field sites in central Italy. Fares et al. (2006) reported that O_3 exposure for 30 days with 150 ppb (11 h per day) induced O_3 visible injury in white poplar. The ambient level of O_3 concentration may not have been high enough to cause the visible injury on white poplar leaves. However, relatively high POD_0 was found in white poplar (44–47 mmol m^{-2} during May–September), which exceeded the CL of POD_0 for Oxford poplar clone (26 mmol m^{-2}). The stomatal flux-based CL for the O_3 visible injury may be species-specific (Günthardt-Goerg et al. 2000; Sicard et al. 2016). This difference of the sensitivity to O_3 between poplar species could be interpreted as lower $\Sigma U/P_n$ values in white poplar than Oxford clone (Table S1; ~1.0 mol mol^{-1} in white poplar, and 1.3–2.8 mol mol^{-1} in Oxford clone during May–September). Biochemical detoxification capacity may be related to leaf mass per area (LMA) because greater LMA implies a higher density of mesophyll tissues (Wieser et al. 2002). Higher LMA values are associated with higher antioxidant content per leaf area in 29 deciduous and evergreen tree species in China (Li et al. 2016). In fact, white poplar leaves had higher LMA values (80.0 g m^{-2}) than the leaves of Oxford poplar clone (70.0 g m^{-2}). The results indicate that white poplar might have a relatively higher detoxification capacity to O_3 than Oxford clone.

To calculate the O_3 indices, we provided the parameterization of the stomatal conductance and photosynthesis models for these poplar species. The model estimation of g_{sw} and P_n showed good agreement with the measurement values (R^2 = 0.72 to 0.83) (Table 4). This result is comparable with previous results of Jarvis-type modeling in tree species (Uddling et al. 2005; Alonso et al. 2008; Hoshika et al. 2012b). In the parameterization, Tuovinen et al. (2007) highlighted the importance of g_{max} in determining the uptake of O_3 by stomata. Values of g_{max} in our study were within the range of previous observations of g_{max} in Oxford clone (450 to 870 mmol m^{-2} s^{-1}; e.g., Marzuoli et al. 2009; Desotgiu et al. 2013; Pollastrini et al. 2014) and white poplar (250 to 500 mmol m^{-2} s^{-1}; e.g., Bernacchi et al. 2003; Fares et al. 2006; Brilli et al. 2007). Similarly, the values of light-saturated net photosynthetic rate, A_{sat} ($\approx P_{max} - R$), were consistent with previous observations in Oxford clone (11 to 17 μmol m^{-2} s^{-1}; e.g., Desotgiu et al. 2013; Pollastrini et al. 2014) and white poplar (17 to 25 μmol m^{-2} s^{-1}; e.g., Bernacchi et al. 2003; Fares et al. 2006; Brilli et al. 2007). In our study, the stomatal conductance and photosynthesis models were separately parameterized because O_3 may often cause a decoupling of stomatal conductance from photosynthesis (Lombardozzi et al. 2012; Hoshika et al. 2013b). Such a response might be related to O_3-induced less efficient stomatal control, i.e., stomatal sluggishness (Paoletti and Grulke 2010). Our results indicate differential responses of photosynthesis and stomatal conductance to O_3 (Fig. 1). The larger reductions of photosynthesis by O_3 imply that the defense capacity in the O_3-injured leaves declined, even though stomatal O_3 uptake was limited due to a reduction of stomatal conductance.

Based on the results of present study, we conclude that our hypothesis was supported, i.e., a more mechanistic approach using stomatal O_3 flux explained the onset of O_3 visible injury better than AOT40. We tried for the first time to extend the results of O_3 visible injury from O_3 FACE experimental studies. We suggested 19 ppm h AOT40, 26 mmol m^{-2} POD_0, and 1.2 mol mol^{-1} $\Sigma U/P_n$ as CLs of O_3 visible injury for this O_3-sensitive poplar clone. The best metric to explain O_3 visible injury onset was $\Sigma U/P_n$. Our result suggests that O_3 visible injury may finally occur in poplars when stomatal O_3 uptake exceeds a critical range of the tolerance due to the assimilate availability for repair and defense against O_3 stress. For a mechanistic understanding of the O_3 effects, both O_3 uptake into a leaf and the capacity for repair and detoxification should be considered (Musselman and Massman 1999).

Acknowledgements We would like to thank Moreno Lazzara for support during the field work, the Fondazione Cassa di Risparmio di Firenze (2013/7956) and the LIFE15 ENV/IT/000183 project MOTTLES for financial support to the experiment, and the National Natural Science Foundation of China (31401895) and China Scholarship Council (201606615002) for financial support to Lu Zhang for his visiting research in Italy.

References

Alonso R, Elvira S, Sanz MJ, Gerosa G, Emberson LD, Bermejo B, Gimeno BS (2008) Sensitivity analysis of a parameterization of the stomatal component of the DO_3SE model for *Quercus ilex* to estimate ozone fluxes. Environ Pollut 155:473–480

Ball JT, Woodrow IE, Berry JA (1987) A model predicting stomatal conductance and its contribution to the control of photosynthesis

under different environmental conditions. Progress in Photosynthesis Research (ed. By J. Biggens), pp.221–224. Martinus-Nijhoff Publishers, Dordrecht.

Baumgarten M, Werner H, Häberle K-H, Emberson LD, Fabian P, Matyssek R (2000) Seasonal ozone response of mature beech trees (*Fagus sylvatica*) at high altitude in the Bavarian forest (Germany) in comparison with young beech grown in the field and in phytotrons. Environ Pollut 109:431–442

Bernacchi CJ, Calfapietra C, Davey PA, Wittig VE, Scarascia-Mugnozza GE, Raines CA, Long SP (2003) Photosynthesis and stomatal conductance responses of poplars to free-air CO_2 enrichment (PopFACE) during the first growth cycle and immediately following coppice. New Phytol 159:609–621

Brilli F, Barta C, Fortunati A, Lerdau M, Loreto F, Centritto M (2007) Response of isoprene emission and carbon metabolism to drought in white poplar (*Populus alba*) saplings. New Phytol 175:244–254

Carriero G, Emiliani G, Giovannelli A, Hoshika Y, Manning WJ, Traversi ML, Paoletti E (2015) Effects of long-term ambient ozone exposure on biomass and wood traits in poplar treated with ethylenediurea (EDU). Environ Pollut 206:575–581

CLRTAP (2015) Mapping critical levels for vegetation, Chapter III of Manual on methodologies and criteria for modelling and mapping critical loads and levels and air pollution effects, risks and trends. UNECE Convention on Long-range Transboundary Air Pollution. http://icpmapping.org/Publications_CLRTAP. Accessed 20 March 2017

Desotgiu R, Pollastrini M, Cascio C, Gerosa G, Marzuoli R, Bussotti F (2013) Responses to ozone on *Populus* "Oxford" clone in an open top chamber experiment assessed before sunrise and in full sunlight. Photosynthetica 51:267–280

Fares S, Barta C, Brilli F, Centritto M, Ederli L, Ferranti F, Pasqualini S, Reale L, Tricoli D, Loreto F (2006) Impact of high ozone on isoprene emission, photosynthesis and histology of developing *Populus alba* leaves directly or indirectly exposed to the pollutant. Physiol Plant 128:456–465

Fares S, Mahmood T, Liu S, Loreto F, Centritto M (2011) Influence of growth temperature and measuring temperature on isoprene emission, diffusive limitations of photosynthesis and respiration in hybrid poplars. Atmos Environ 45:155–161

Feng Z, Sun J, Wan W, Hu E, Catalayud V (2014) Evidence of widespread ozone-induced visible injury on plants in Beijing, China. Environ Pollut 193:296–301

Fredericksen TS, Kolb TE, Skelly JM, Steiner KC, Joyce BJ, Savage JE (1996) Light environment alters ozone uptake per net photosynthetic rate in black cherry trees. Tree Physiol 16:485–490

Günthardt-Goerg MS, McQuattie CJ, Maurer S, Frey B (2000) Visible and microscopic injury in leaves of five deciduous tree species related to current critical ozone levels. Environ Pollut 109:489–500

Haagen-Smit AJ, Darley EF, Zaitlin M, Hull H, Noble W (1952) Investigation on injury to plants from air pollution in the Los Angeles area. Plant Physiol 27:18–34

Hartmann DL, Klein Tank AMG, Rusticucci M, Alexander LV, Brönnimann S, Charabi Y, Dentener FJ, Dlugokencky EJ, Easterling DR, Kaplan A, Soden BJ, Thorne PW, Wild M, Zhai PM (2013) Observations: atmosphere and surface. In: Stocker TF, Qin D, Plattner GK, Tignor M, Allen SK, Boschung J, Nauels A, Xia Y, Bex V, Midgley PM (eds) Climate Change 2013: The Physical Science Basis. Contribution of Working Group I to the Fifth Assessment Report of the Intergovernmental Panel on Climate Change. Cambridge University Press, Cambridge, pp 159–254

Hoshika Y, Paoletti E, Omasa K (2012a) Parameterization of *Zelkova serrata* stomatal conductance model to estimate stomatal ozone uptake in Japan. Atmos Environ 55:271–278

Hoshika Y, Watanabe M, Inada N, Koike T (2012b) Modeling of stomatal ozone conductance for estimating ozone uptake of *Fagus crenata* under experimentally enhanced free-air ozone exposure. Water Air Soil Pollut 223:3893–3901

Hoshika Y, Omasa K, Paoletti E (2012c) Whole-tree water use efficiency is decreased by ambient ozone and not affected by O_3-induced stomatal sluggishness. PLoS One 7:e39270

Hoshika Y, Pecori F, Conese I, Bardelli T, Marchi E, Manning WJ, Badea O, Paoletti E (2013a) Effects of a three-year exposure to ambient ozone on biomass allocation in poplar using ethylenediurea. Environ Pollut 180:299–303

Hoshika Y, Watanabe M, Inada M, Koike T (2013b) Model-based analysis of avoidance of ozone stress by stomatal closure in Siebold's beech (*Fagus crenata*). Ann Bot-London 112:1149–1158

Hoshika Y, Carriero G, Zhaozhong F, Zhang Y, Paoletti E (2014) Determinants of stomatal sluggishness in ozone-exposed deciduous tree species. Sci Total Environ 481:453–468

Iio A, Fukasawa H, Nose Y, Kakubari Y (2004) Stomatal closure induced by high vapor pressure deficit limited midday photosynthesis at the canopy top of *Fagus crenata* Blume on Naeba Mountain in Japan. Trees 18:510–517

Innes JL, Skelly JM, Schaub M (2001) Ozone and broadleaved species. A guide to the identification of ozone-induced foliar injury, Paul Haupt Verlag Bern

Jarvis PG (1976) Interpretation of variations in leaf water potential and stomatal conductance found in canopies in field. Philos Trans R Soc B 273:593–610

Kolb TE, Matyssek R (2001) Limitation and perspectives about scaling ozone impacts in trees. Environ Pollut 115:373–393

Körner C (1995) Leaf diffusive conductances in the major vegetation types of the globe. In: Schulze ED, Caldwell MM (eds) Ecophysiology of Photosynthesis. Ecological Studies Vol. 100. Springer, Heidelberg, pp 463–490

Li P, Catalayud V, Gao F, Uddling J, Feng Z (2016) Differences in ozone sensitivity among woody species are related to leaf morphology and antioxidant levels. Tree Physiol 36:1105–1116

Lombardozzi D, Sparks JP, Bonan G, Levis S (2012) Ozone exposure causes a decoupling of conductance and photosynthesis: implications for the Ball-Berry stomatal conductance model. Oecologia 169:651–659

Marzuoli R, Gerosa G, Desotgiu R, Bussotti F, Ballarin-Denti A (2009) Ozone fluxes and foliar injury development in the ozone-sensitive poplar clone Oxford (*Populus maximowiczii* x *Populus berolinensis*). Tree Physiol 29:67–76

Massman WJ (2004) Toward an ozone standard to protect vegetation based on effective dose: a review of deposition resistances and a possible metric. Atmos Environ 38:2323–2337

Matyssek R, Sandermann H, Wieser G, Booker F, Cieslik S, Musselman R, Ernst D (2008) The challenge of making ozone risk assessment for forest trees more mechanistic. Environ Pollut 156:567–582

Matyssek R, Clarke N, Cudlin P, Mikkelsen TN, Tuovinen JP, Wieser G, Paoletti E (2013) Climate change, air pollution and global challenges: understanding and perspectives from forest research. Developments in Environmental Science 13. Elsevier, Amsterdam

Middleton JT, Kendrick JB, Schwalm HW (1950) Smog in the south coastal area of California. Calif Agric 4(11):7–10

Middleton JT, Kendrick JB, Darley EF (1953) Air pollution injury to crops. Calif Agric 7(1):11–12

Middleton JT, Crafts AS, Brewer RF, Taylor OC (1956) Plant damage by air pollution. Calif Agric 10(6):9–12

Moura BB, Alves ES, de Souza SR, Domingos M, Vollenweider P (2014) Ozone phytotoxic potential with regard to fragments of the Atlantic semi-deciduous forest downwind of Sao Paulo, Brazil. Environ Pollut 192:65–73

Muraoka H, Tang Y, Terashima I, Koizumi H, Washitani I (2000) Contributions of diffusional limitation, photoinhibition and photorespiration to midday depression of photosynthesis in *Arisaema heterophyllum* in natural high light. Plant Cell Environ 23:235–250

Musselman RC, Massman WJ (1999) Ozone flux to vegetation and its relationship to plant response and ambient air quality standards. Atmos Environ 33:65–73

Noble WM (1955) Pattern of damage produced on vegetation by smog. Agric Food Chem 3:330–332

Noctor G, Foyer C (1998) Ascorbate and glutathione: keeping active oxygen under control. Annu Rev Plant Physiol 49:249–279

Novak K, Skelly JM, Schaub M, Kräuchi N, Hug C, Landolt W, Bleuler P (2003) Ozone air pollution and foliar injury development on native plants of Switzerland. Environ Pollut 125:41–52

Oue H, Kobayashi K, Zhu J, Guo W, Zhu X (2011) Improvements of the ozone dose response functions for predicting the yield loss of wheat due to elevated ozone. J Agric Meteorol 67:21–32

Paoletti E, Grulke N (2010) Ozone exposure and stomatal sluggishness in different plant physiognomic classes. Environ Pollut 158:2664–2671

Paoletti E, Manning WJ (2007) Toward a biologically significant and usable standard for ozone that will also protect plants. Environ Pollut 150:85–95

Paoletti E, Contran N, Manning WJ, Ferrara AM (2009a) Use of the antiozonant ethylenediurea (EDU) in Italy: verification of the effects of ambient ozone on crop plants and trees and investigation of EDU's mode of action. Environ Pollut 157:1453–1460

Paoletti E, Ferrara AM, Calatayud V, Cervero J, Giannetti F, Sanz MJ, Manning WJ (2009b) Deciduous shrubs for ozone bioindication: *Hibiscus syriacus* as an example. Environ Pollut 157:865–870

Paoletti E, Contran N, Bernasconi P, Günthardt-Goerg MS, Vollenweider P (2009c) Structural and physiological responses to ozone in Manna ash (*Fraxinus ornus* L.) leaves in seedlings and mature trees under controlled and ambient conditions. Sci Total Environ 407:1631–1643

Paoletti E, Materassi A, Fasano G, Hoshika Y, Carriero G, Silaghi D, Badea O (2017) A new-generation 3D ozone FACE (free air controlled exposure). Sci Tot Environ 575:1407–1414

Peel MC, Finlayson BL, McMahon TA (2007) Updatedworld map of the Köppen-Geiger climate classification. Hydrol Earth Syst Sci 11:633–1644

Pihl Karlsson G, Sellden G, Skarby L, Pleijel H (1995) Clover as an indicator plant for phytotoxic ozone concentrations: visible injury in relation to species, leaf age and exposure dynamics. New Phytol 129(2):355–365

Pihl Karlsson G, Karlsson PE, Soja G, Vandermeiren K, Pleijel H (2004) Test of the short-term critical levels for acute ozone injury on plants-improvements by ozone uptake modelling and the use of an effect threshold. Atmos Environ 38:2237–2245

Pollastrini M, Desotgiu R, Camin F, Ziller L, Gerosa G, Marzuoli R, Bussotti F (2014) Severe drought events increase the sensitivity to ozone on poplar clones. Environ Exp Bot 100:94–104

Richards BL, Middleton JT, Hewitt WB (1958) Air pollution with relation to agronomic crops. V. Oxidant stipple of grape. Agron J 50:559–561

Sicard P, De Marco A, Dalstein-Richier L, Tagliaferro F, Paoletti E (2016) An epidemiological assessment of stomatal ozone flux-based critical levels for visible ozone injury in Southern European forests. Sci Total Environ 541:729–741

Smirnoff N (1996) The function and metabolism of ascorbic acid in plants. Ann Bot-London 78:661–669

Tuovinen J-P, Simpson D, Emberson L, Ashmore M, Gerosa G (2007) Robustness of modelled ozone exposures and doses. Environ Pollut 146:578–586

Uddling J, Hall M, Wallin G, Karlsson PE (2005) Measuring and modelling stomatal conductance and photosynthesis in mature beech in Sweden. Agric For Meteorol 132:115–131

Van der Heyden D, Skelly J, Innes J, Hug C, Zhang J, Landolt W, Bleuler P (2001) Ozone exposure thresholds and foliar injury on forest plants in Switzerland. Environ Pollut 111:321–331

Watanabe M, Hoshika Y, Inada N, Koike T (2014) Canopy carbon budget of Siebold's beech (*Fagus crenata*) sapling under free air ozone exposure. Environ Pollut 184:682–689

Wieser G, Tegischer K, Tausz M, Häberle K-H, Grams TEE, Matyssek R (2002) Age effects on Norway spruce (*Picea abies*) susceptibility to ozone uptake: a novel approach relating stress avoidance to defense. Tree Physiol 22:583–590